International Journal of Chemical, Materials and Biomolecular Sciences
ISSN: 2415-6620
Vol:13, No:6, 2019

A Composite Developed from a Methyl Methacrylate and Embedded Eppawala Hydroxyapatite for Orthopedics

H. K. G. K. D. K. Hapuhinna, R. D. Gunaratne, H. M. J. C. Pitawala

***Abstract*—**This study aimed to find out chemical and structural suitability of synthesized eppawala hydroxyapatite composite as bone cement, by comparing and contrasting it with human bone as well as commercially available bone cement, which is currently used in orthopedic surgeries. Therefore, a mixture of commercially available bone cement and its liquid monomer, commercially available methyl methacrylate (MMA) and a mixture of solid state synthesized eppawala hydroxyapatite powder with commercially available MMA were prepared as the direct substitution for bone cement. Then physical and chemical properties including composition, crystallinity, presence of functional groups, thermal stability, surface morphology, and microstructural features were examined compared to human bone. Results show that there is a close similarity between synthesized product and human bone and it has exhibited high thermal stability, good crystalline and porous properties than the commercial product. Finally, the study concluded that synthesized hydroxyapatite composite can be used directly as a substitution for commercial bone cement.

***Keywords*—**Hydroxyapatite, bone cement, methyl methacrylate, orthopedics.

I. Introduction

EPPAWALA choloroapatite deposit is one of the nonrenewable phosphate sources situated in Anuradhapura, ancient capital of Sri Lanka which usually contains 34-40% total phosphorus expressed as percentage of phosphorus pentoxide (P_2O_5) [1]-[5]

Among so many phosphate products, up to the date eppawala chloroapatite mineral is only considered as the raw material for fertilizer industry. Therefore, hydroxyapatite, a well-known bioceramic is prepared as value addition to eppawala chloroapatite using solid state sintering method. For that, ability of replacing chloroapatite's chlorine with other groups at high temperature due to the increase of reactivity was considered as its chlorine positions are under strain in the structural framework [2], [3].

Hydroxyapatite is a widely used bioceramic which has a close chemical and structural similarity with human hard tissues and performs several outstanding properties; biocompatibility, non-inflammatory in nature, osteoconductivity, non-toxicity, bioactivity etc. [6]-[11]. As a result it has a range of biomedical applications mainly in the fields of orthopedics and dentistry [12]-[25].

This study mainly focused to find out the suitability of solid-state sintered eppawala hydroxyapatite with MMA monomer as bone cement, by comparing and contrasting it with human bone as well as commercially available bone cement, which is currently used in orthopedic surgeries.

Selected commercial product containing two main parts as bone cement majorly consists of zirconium dioxide and a liquid monomer MMA. Currently, it is used as fast curing bone cement in Sri Lankan government hospitals which indicates for stable attachment of total or partial joint endoprostheses in bone, filling and stabilization bone defects within the scope of internal fixation treatment or for endoprosthesis revision surgery and primary and secondary coverage of skull bone defects. It is prepared directly before use by mixing its powder component with liquid monomer component clinically. Resulted ductile dough is cured within a few minutes [26].

Research designed to explore the possibility of substituting synthesized ceramic powder into cement powder of commercial product. Therefore, both synthesized powder and commercial product were mixed with Methyl Methacrylate (MMA) liquid monomer and only find out structural suitability of ceramic product as bone cement.

II. Experimental Procedure

A. Sample Preparation

As the first step, Solid State Sintered Eppawala Hydroxyapatite (SSHAp) was prepared using solid state sintering method. Purified eppawala chloroapatite or high grade rock phosphate and calcium hydroxide was used as the raw materials [2], [17]:

$$Ca(OH)_{2(s)} + 2Ca_5(PO_4)_3Cl_{(s)} \xrightarrow{\text{High temperatures, (10-12) hrs}} 2Ca_5(PO_4)_3OH_{(s)} + CaCl_{2(s)}$$

Then the synthesized ceramic powder was mixed with MMA liquid monomer, which came with the commercial product until the ductile dough forms. As the second step, commercial cement powder and liquid monomer were mixed together until the ductile dough forms.

H. K. G. K. D. K. Hapuhinna is with the Department of Engineering Technology, Faculty of Technology, University of Sri Jayewardenepura, Sri Lanka (e-mail: khapuhinna@ymail.com).

R. D. Gunaratne is with the Department of Engineering Technology, Faculty of Technology, University of Sri Jayewardenepura, Sri Lanka (corresponding author, e-mail: rajitha@sjp.ac.lk).

H. M. J. C. Pitawala is with the Department of Science & Technology, Faculty of Science & Technology, Uva Wellassa University, Sri Lanka (e-mail: jcpitawala@yahoo.com).

B. Sample Characterization

Before mixing with the liquid monomer; commercial bone cement and Eppawala Hydroxyapatite were examined under X-ray fluorescence Spectroscopy (Rigaku XRF Spectrometer) to find out its elementary composition and presence of impurities. Liquid monomer was examined with Fourier Transform Infrared Spectroscopy (Bruker – Alpha FTIR Spectroscopy) ATR mode to confirm its composition. Then sample mixture of newly prepared bone cement and the sample mixture of commercial bone cement were characterized using XRD, FTIR, TGA, and SEM with EDS techniques together with the human bone sample. The crystallographic phases of samples were determined by X- ray diffractometer (Rigaku – Ultima. IV diffractometer) in reflection mode with Cu Kα1: 0.154 nm radiation. 1.5^0 min^{-1} scanned speed was used to collect data within a 2θ range from 15^0 to 80^0. The presence of functional groups was confirmed by using Fourier Transform Infrared Spectroscopy (Bruker – Alpha FTIR Spectroscopy). The FTIR spectra were obtained over the region 400-4000 cm^{-1} using KBr pellet technique. The resolution of the spectrometer was 4 cm^{-1}. The surface morphology and microstructural features of samples were studied using Hitachi SU6600 Analytical Variable Pressure FE-SEM (Field Emission Scanning Electron Microscope) and Oxford Instruments EDX with AZtec software. Furthermore, Thermogravimetric analysis (TGA) was done using a Thermal Analyzer (SDT Q600) with N environment, 10 ^0C min^{-1} heating rate, and 1450 ^0C maximum temperature to find out the thermal stability of samples.

III. Results and Discussion

A. XRF Analysis

TABLE I
XRF Results for Commercial Bone Cement

Element	Spot 1	Spot 2	Spot 3	Spot 4	Spot 5	Spot 6
	Mass %	Mass %	Mass %	Mass %	Mass %	Mass %
16 S	8.84	-	-	10.32	-	-
40 Zr	87.65	96.19	96.43	86.00	96.56	96.45
72 Hf	3.51	3.81	3.57	3.67	3.44	3.55

Table I shows that commercial bone cement sample contains Zr and S present in higher amounts and Hf in fewer amounts. When comparing to the literature, there is a difference between commercial bone cement with bone ash meal, as it contains 54.14% CaO, 38.03% P_2O_5 and 0 to 0.9% Fe_2O_3, SiO_2, Al_2O_3 [26] and previous research findings show that SSHAp and bone ash has a similarity in composition [2], [17].

B. SEM with EDS Analysis

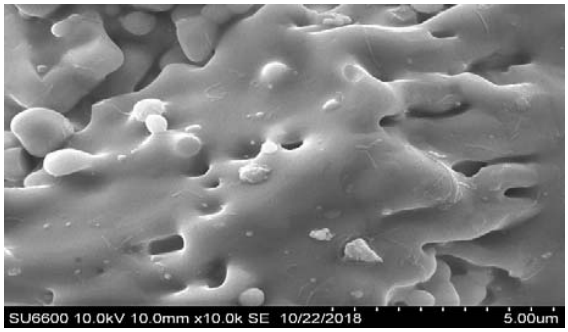

(a)

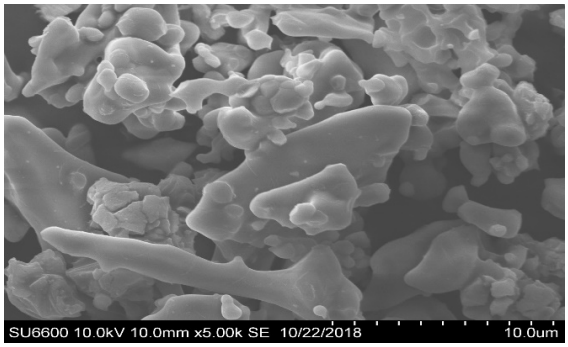

(b)

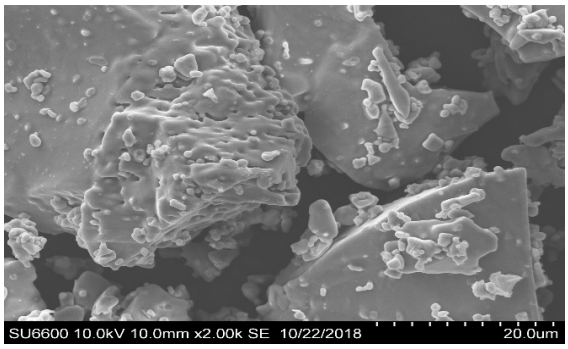

(c)

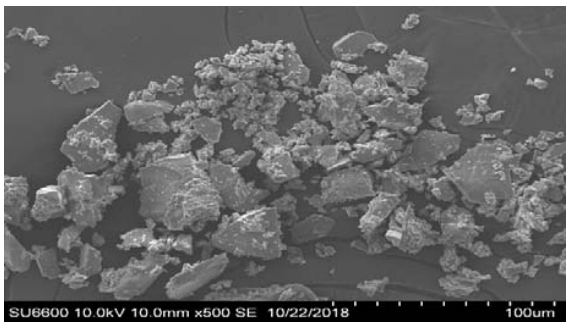

(d)

Fig. 1 SEM images for SSHAp ceramic+ MMA mixture, 10.0 kv, (a) 10K (b) 5KX (c) 2KX (d) 500X

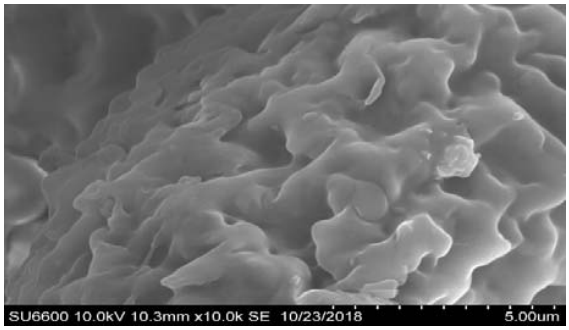

(e)

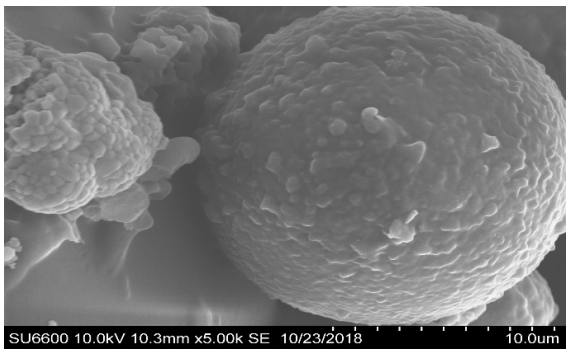

(f)

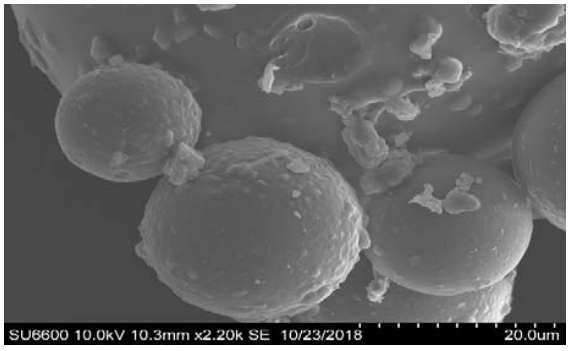

(g)

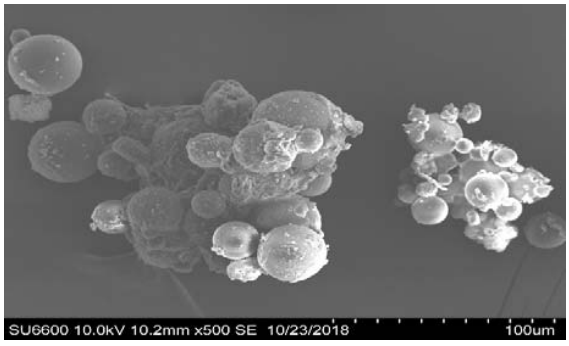

(h)

Fig. 2 SEM images for Commercial bone cement + MMA mixture, 10.0 kv, (e) 10K (f) 5KX (g) 2.2KX (h) 500X

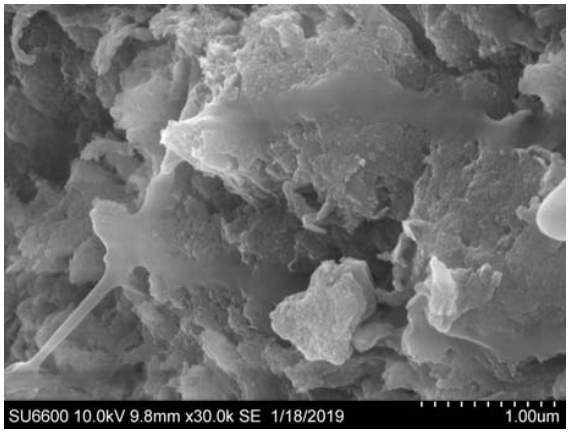

(i)

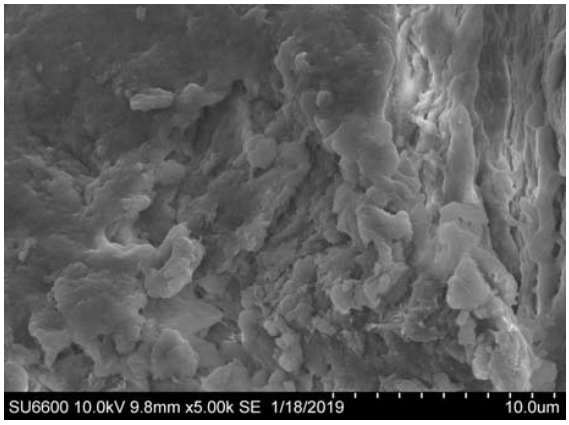

(j)

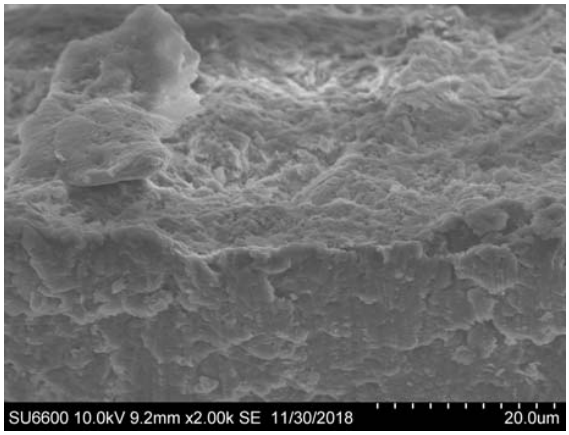

(k)

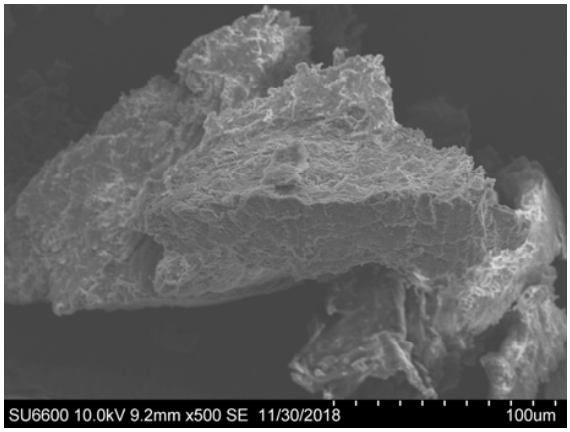

(l)

Fig. 3 SEM images for Human bone, 10.0 kv, (i) 30KX (j) 5KX (k) 2KX (l) 500X

Considering Figs. 1-3, SEM images of all mixtures and human bone show that there are good correlations of particles. Both human bone and sample mixture of SSHAp and MMA consist of micropores as shown in Fig. 1. Porosity would be helpful for bone ingrowth as well as for good blood circulation. Presence of some spherical shaped particles with rough surface, were found in commercial bone cement mixture which may lead to have higher surface area as mentioned in Fig. 2. According to Fig. 3, some crystalline property can be found in both human bone and SSHAp with MMA mixture.

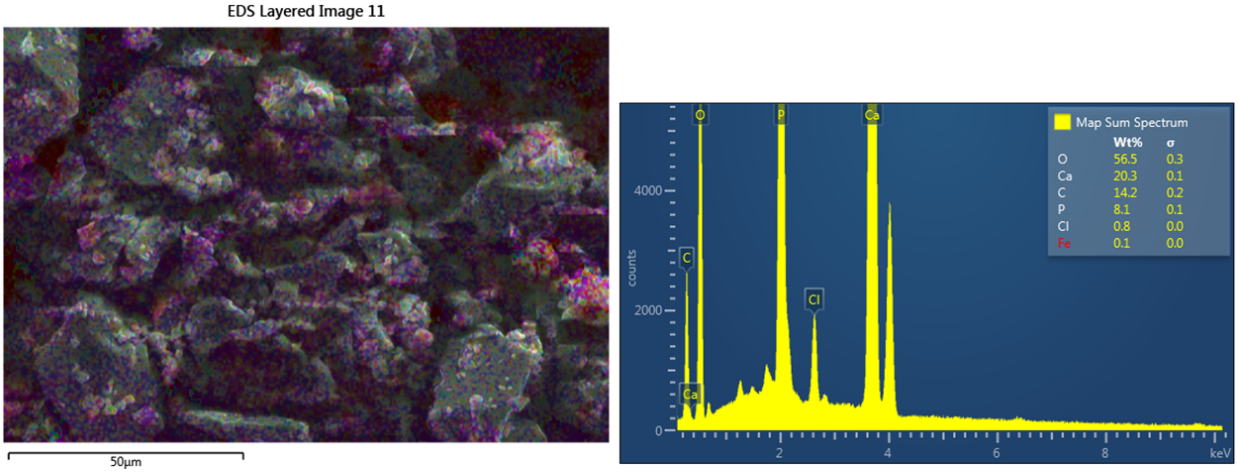

(a1)

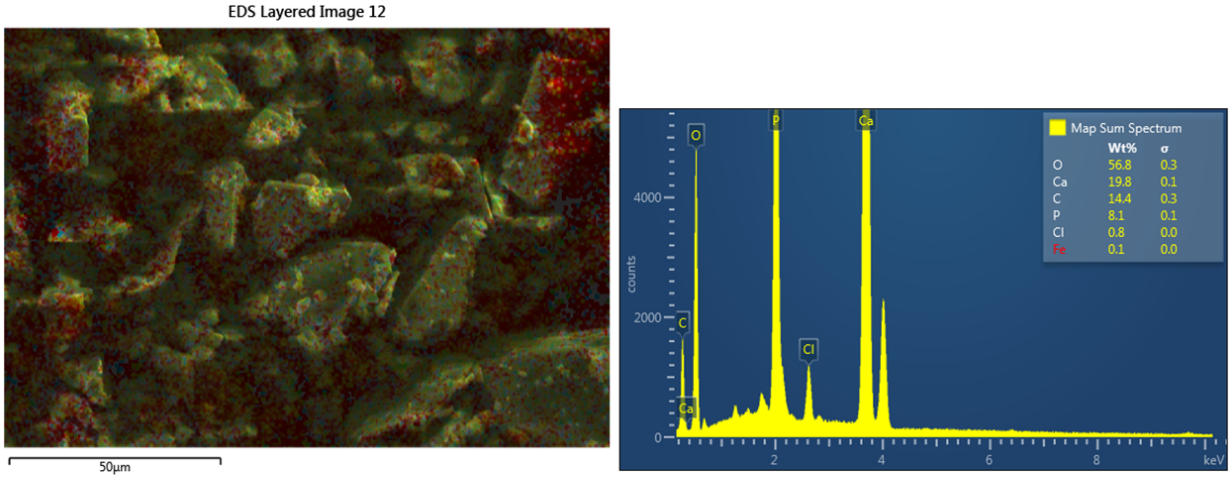

(b1)

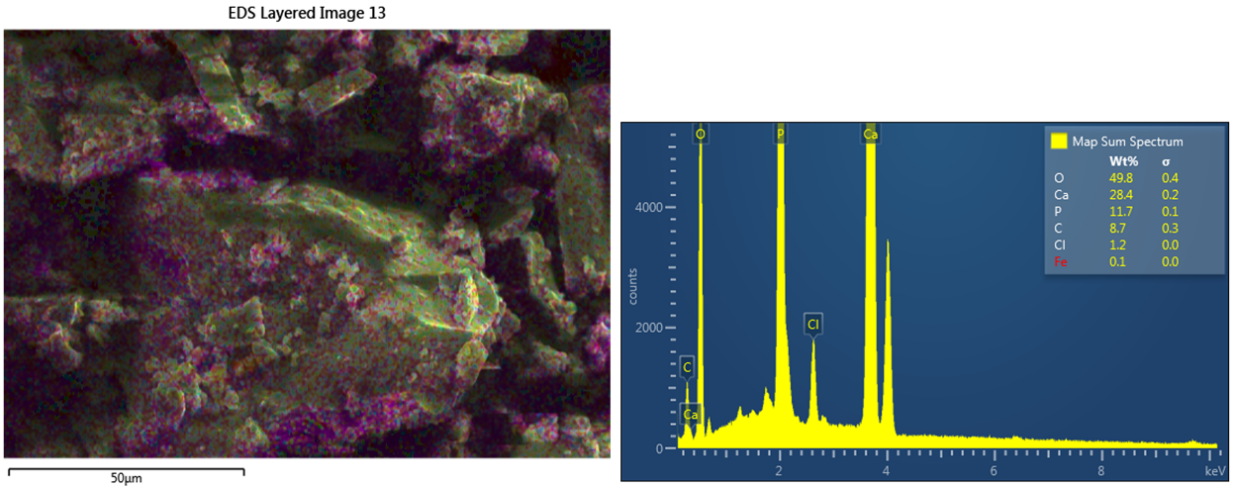

(c1)

Fig. 4 SEM with EDS images for SSHAp with liquid monomer mixture

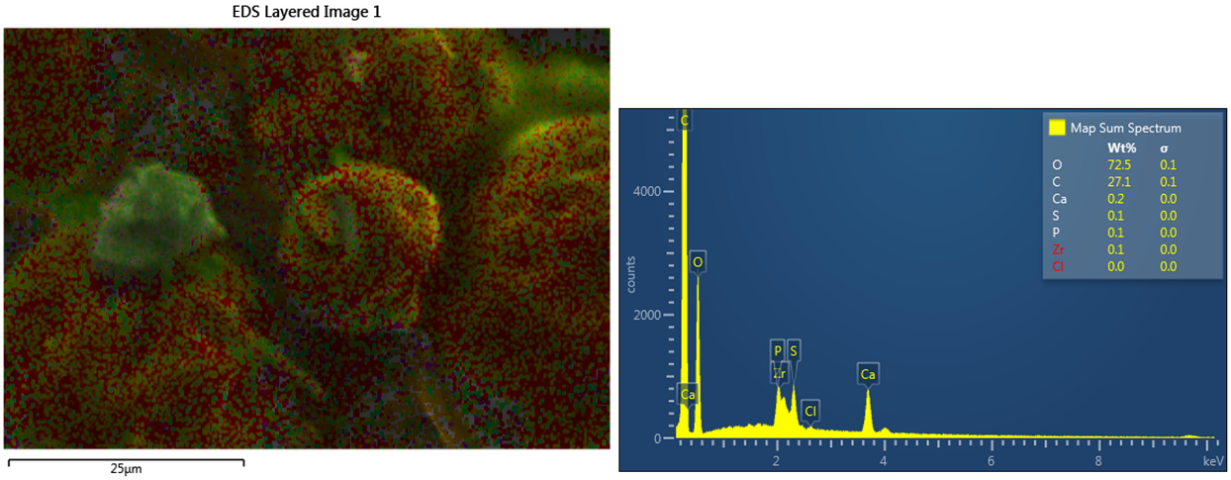

(a2)

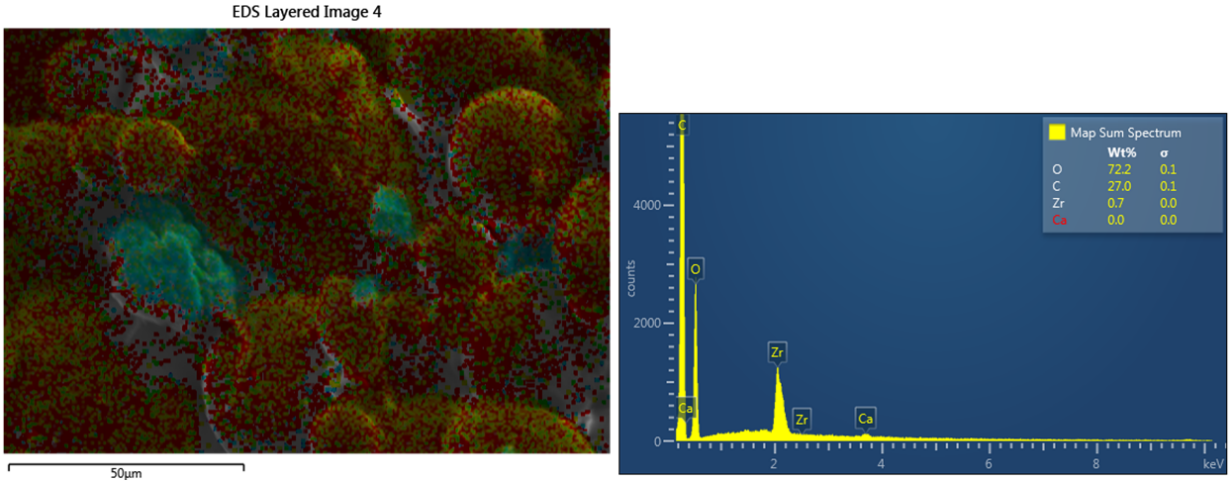

(b2)

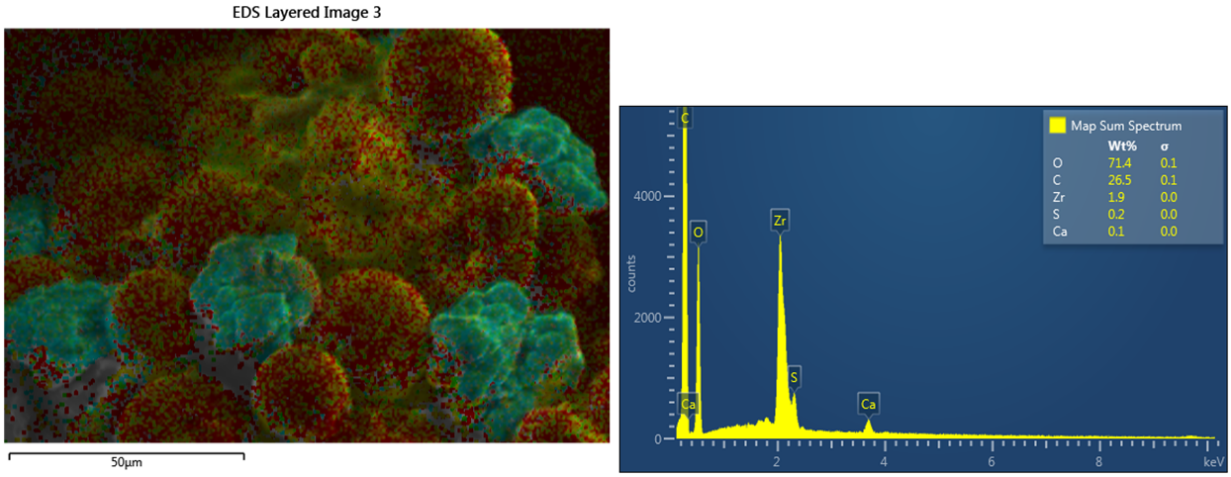

(c2)

Fig. 5 SEM with EDS images for Commercial bone cement with liquid monomer mixture

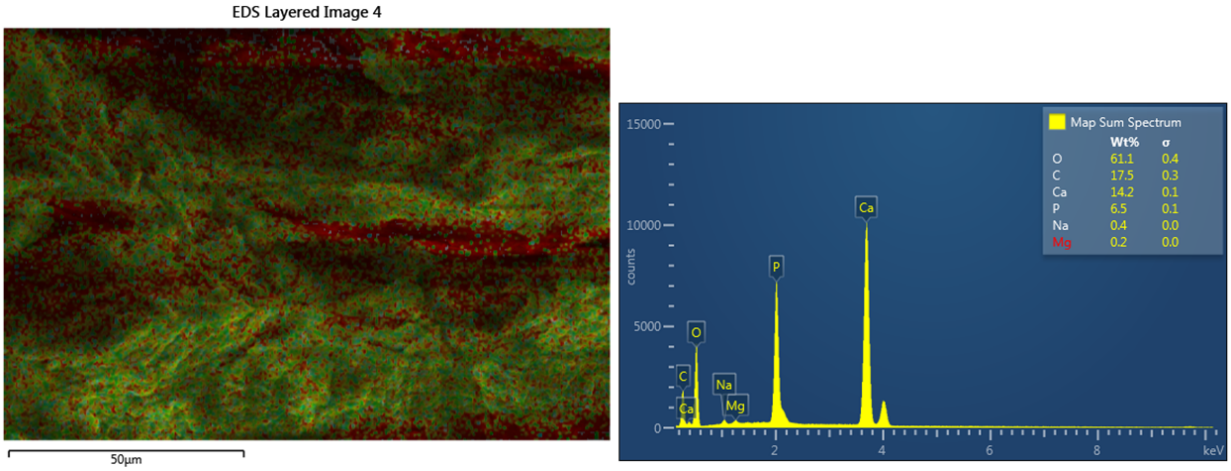

(a3)

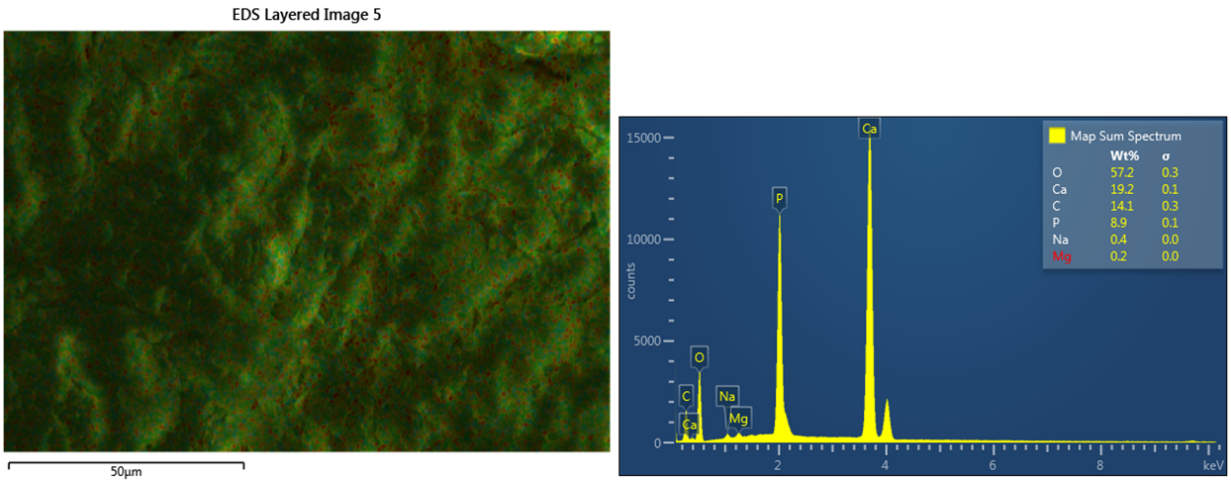

(b3)

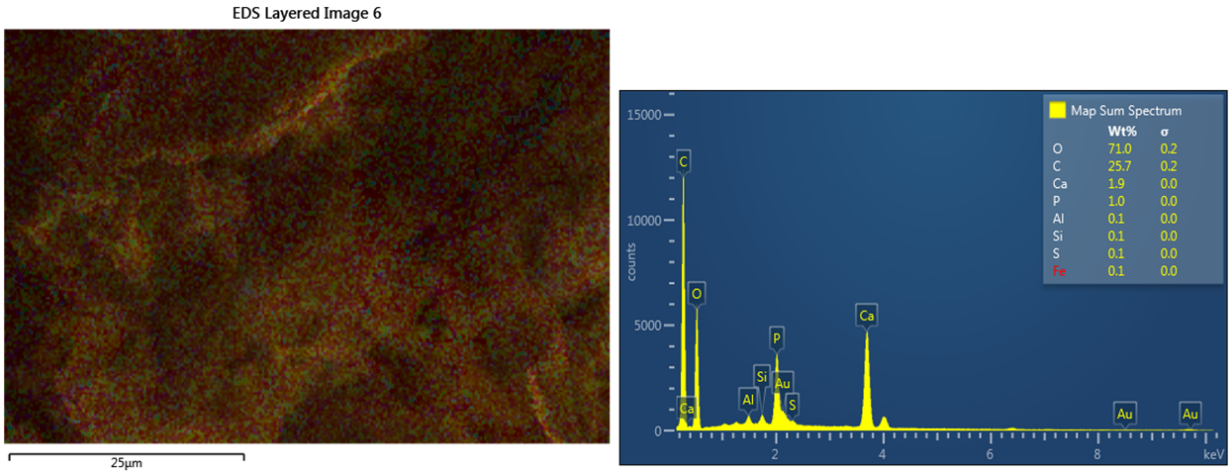

(c3)

Fig. 6 SEM with EDS images for Human bone

As indicated in Fig. 4, SEM with EDS images of SSHAp with MMA mixture show that sample contains O, Ca in higher amounts and then P, C, Cl in order. Fe is also found in very less amount as an impurity. Commercial product mixture contains O, C in higher amounts of the products and in order Ca, Zr, S, and P according to Fig. 5. Fig. 6 interprets that the human bone contains O as the highest amount and then C, Ca, P and Na in descending order. Na, Mg, Al, Si, S, Fe present in very fewer amounts. When comparing results, it can be stated that human bone and the mixture of SSHAp with MMA have similarity in composition.

C. FTIR Analysis

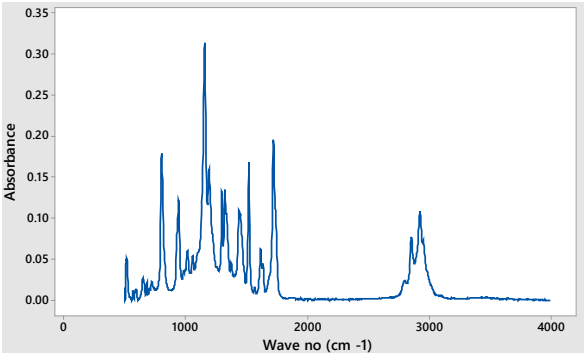

Fig. 7 FTIR graph for liquid monomer

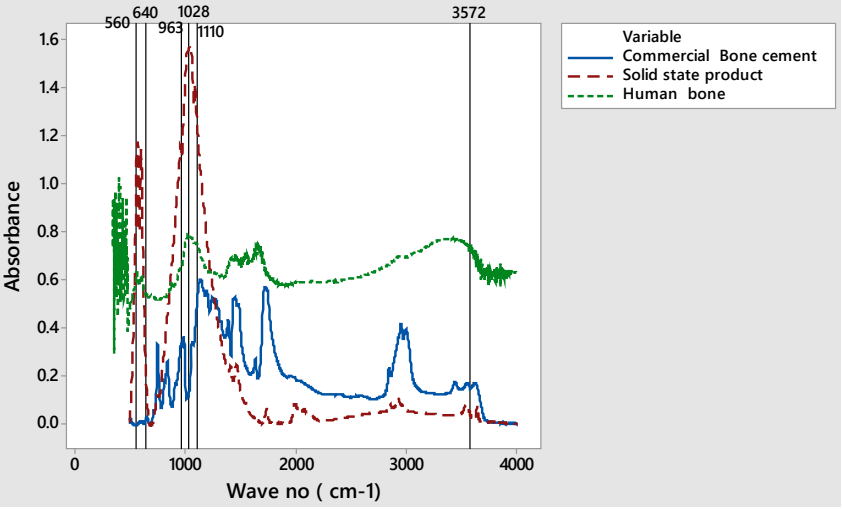

Fig. 8 FTIR comparison for Commercial Bone cement with MMA mixture, SSHAp with MMA mixture and Human bone

Fig. 7 shows the resulted graph for liquid monomer. It has coincided with the FTIR characteristic graph for MMA monomer, therefore liquid monomer in the commercial product was confirmed as the MMA monomer. Presence of peaks near 560 $cm^{-1,}$ 640 cm^{-1}, 963 cm^{-1}, 1028 cm^{-1} and 1110 cm^{-1} wave numbers corresponds to the phosphate groups

included in the product as shown in Fig. 8. Broad peak which appeared in human bone as well as SSHAp with MMA mixture, nearly 3572 cm^{-1} is the characteristic peak for OH^-/ Hydroxyapatite [2], [17]. It confirms the presence of hydroxyapatite in the SSHAp product even after the mixing with a monomer. Even though the commercial product mixture carries peak nearly 3572 cm^{-1} wave number, it could not be identified as the presence of OH^{-1} group related to hydroxyapatite because there is no peaks related to phosphate groups within the mixture. Therefore, it can be assumed that sample may carry moisture. Apart from that, both commercial bone cement with MMA mixture and SSHAp with MMA mixture have common peaks, which could not be found in human bone nearly 750 cm^{-1}- 2000 cm^{-1} and 3000 cm^{-1} wave number range which is also appeared in Fig. 7, they are the related peaks for MMA monomer [27]. As a result, it can be concluded that both commercial bone cement and SSHAp mixed well with the liquid monomer.

D. XRD Analysis

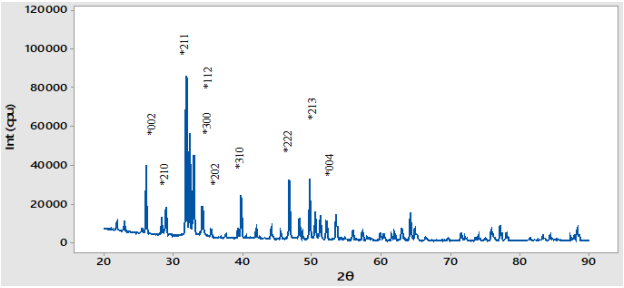

Fig. 9 XRD pattern for SSHAp + MMA mixture

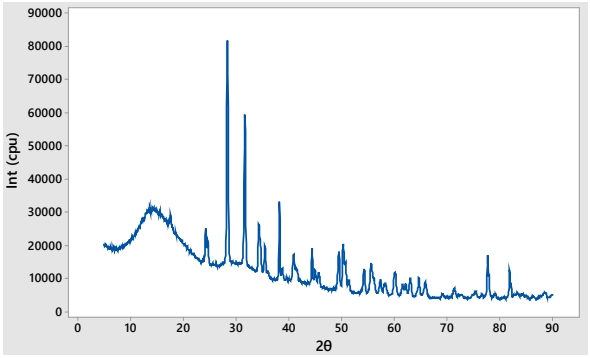

Fig. 10 XRD pattern for Commercial bone cement + MMA mixture

Fig. 9 has shown that SSHAp with MMA sample carries all characteristic peaks related to the crystallographic phases 002, 210, 211, 112, 300, 202, 310, 222, 213 and 004 of hexagonal hydroxyapatite. It shows similarity to human bone [2], [17], [28], [29]. Also, it interprets 96% crystallinlity. Comparing those results with the Fig. 10, XRD pattern for commercial bone cement with MMA monomer, it can be predicted that commercial product also has crystalline properties but its structure does not coincide with hexagonal hydroxyapatite.

E. TGA Analysis

12.9850 mg SSHAp with MMA sample mixture was subjected to TGA as shown in Fig. 11. First significant weight loss which occurs between 100 and 400 ^{0}C (0.2449 mg) representing 1.886% may be associated with the dehydration of the sample. Following that interval the sample reduced its weight nearly 0.1511 mg at 772.07 ^{0}C; it may occur due to the gas elimination. Then again from 772.07 to 1432.97 ^{0}C there is a weight loss indicating 0.45% (0.0584 mg) which has occurred due to the incipient transformation of produced hydroxyapatite into β-TCP. Therefore, it indicates the formation of hydroxyapatite in products. At 1432.97 ^{0}C 96.51 % of the original weight has remained.

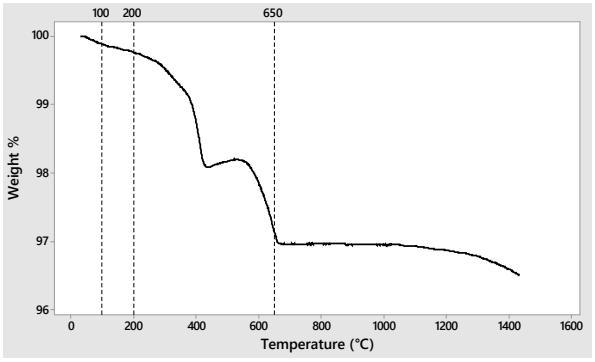

Fig. 11 TGA curve for SSHAP with liquid monomer mixture

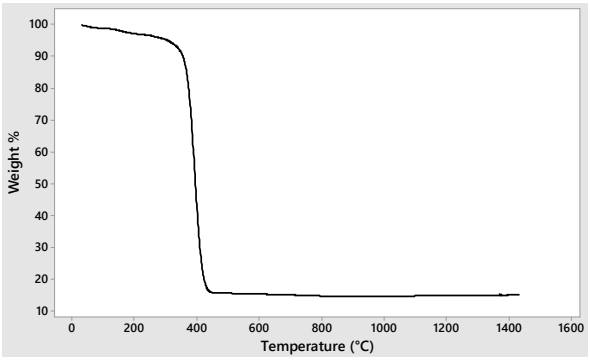

Fig. 12 TGA curve for commercial bone cement with liquid monomer mixture

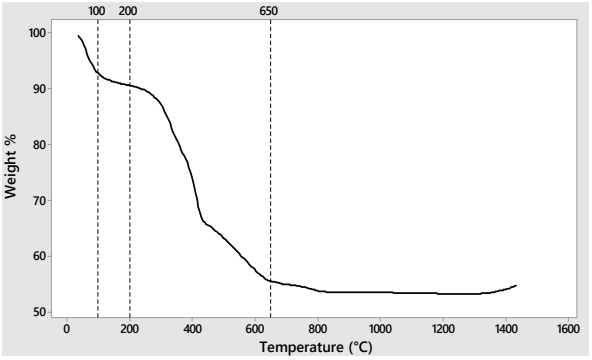

Fig. 13 TGA curve for Human bone

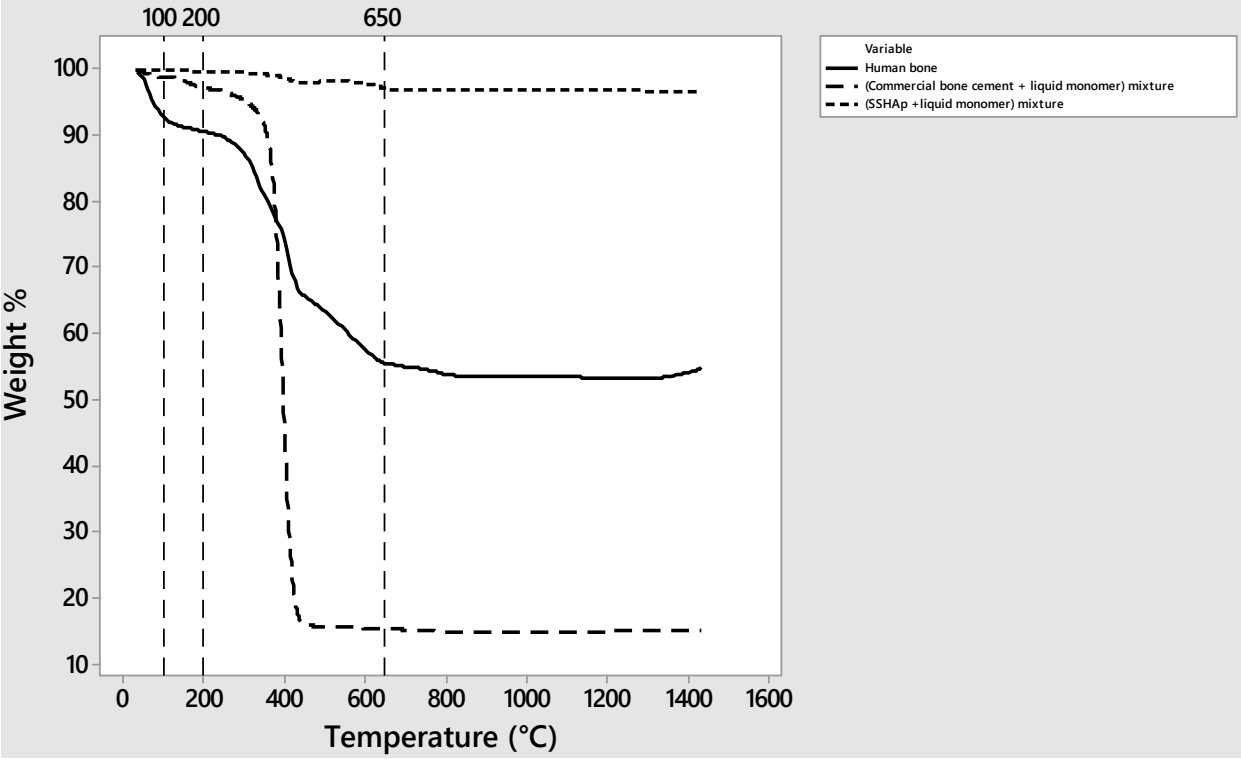

Fig. 14 Comparison between TGA results of Human bone, Commercial bone cement mixture, and Solid state product mixture

14.0710 mg of commercial product mixture was subjected to TGA. Considerable amount of weight loss, 85.14% from initial weight (11.96 mg) was occupied 200 ^{0}C to 400 ^{0}C temperature range. Basically up to 400 ^{0}C weight losses may occur due to the dehydration of samplee/moisture removal. Therefore, it can be predicted that first weight loss may occur due to moisture removal of the product, but there may be some other reasons also such as structural degradation or deformation. Gradually, weight loss rate has become a constant. At the end 1435.98 ^{0}C, 15.23% of initial weight was remained.

According to Fig. 13, 10.115 mg human bone sample was subjected to TGA. As mentioned in [2], [17], [28], [30]; first significant weight loss which occurs nearly at 200 ^{0}C (0.9112 mg) representing 9.008 %, may associate with the dehydration of the sample. Following that interval the sample reduced its weight nearly 5.6358 mg at 650 ^{0}C; it has occurred due to the bone structure collagen elimination. This reaction continues up to 936.88 ^{0}C, with a lowered rate. Above that temperature, a fine TGA curve descending slope is observed up to maximum analyzed temperature of 1432.97 ^{0}C with the total weight loss of 54.79%, this being associated with the collagen remains removal & the incipient transformation of hydroxyapatite in β-TCP [2], [17], [28], [30].

When comparing human bone with commercial bone cement with MMA mixture and SSHAp with MMA mixture, according to Fig. 14, human bone and the SSHAp mixture have shown the same pattern of weight loss, which was slightly different from commercial product mixture. This may happen due to the composition similarity of human bone and SSHAp with MMA monomer mixture, as they were containing hydroxyapatite. Synthesized SSHAp with MMA sample shows very less weight loss compared to human bone and commercial product with MMA samples, therefore it can be concluded that the synthesized SSHAP with MMA monomer mixture performs high thermal stability and good material stability in nature and application

IV. Conclusion

Finally, the study concludes that SSHAp with MMA composite has a chemical and structural similarity with human bone and performs high thermal stability and good material stability in nature. Composite carries 96% crystallinity, microporous structure which leads to osteoconductive properties. Therefore, it can be used as a direct substitution for bone cement.

References

[1] Anon, Eppawala Rock Phosphate Deposit and Processing Plant. Wicky's Blog. Available at: http://slminerals.blogspot.com/2015/09/eppawalarock-phosphate-deposit-and.html (Accessed September 20, 2017).

[2] Hapuhinna, H.; Gunaratne, R.; Pitawala, H. (2018), 'Development of a Biomaterial from Naturally Occurring Chloroapatite Mineral for Biomedical Applications', World Academy of Science, Engineering and Technology, International Science Index 140, International Journal of Chemical, Molecular, Nuclear, Materials and Metallurgical Engineering, 12(8), 380 - 388.

[3] Hapuhinna, H., Gunaratne, R., Pitawala, H., Wijesekara, K. and Ekanayake, E. (2017). Synthesis and characterization of hydroxyapatite from Eppawala Rock Phosphate for Biomedical Applications as a value

added product. (online). Available from: Tradmed International (International Symposium on Traditional and complementary Medicine.
[4] Anon, Industries from Eppawala phosphate deposit. Online edition of Daily News - Features. Available at: http://archives.dailynews.lk/2003/03/07/fea13.html (Accessed September 6, 2017).
[5] Ratnayake, S. P. & Navaratna, A. N., Spectroscopic Determination of Metal Impurities in Commercial Raw Material Fertiliser of Sri Lanka. Researchgate. Available at: https://www.researchgate.net/ (Accessed September 4, 2017).
[6] Kalita SJ, Bhardwaj A, Bhatt HA. Nanocrystalline calcium phosphate ceramics in biomedical engineering. Materials Science and Engineering:C. 2007;27(3):441-9.
[7] M., E. (2011). Hydroxyapatite-Based Materials: Synthesis and Characterization. Biomedical Engineering - Frontiers and Challenges.
[8] V. P., Komlev, V. S. & Barinov, S. M., Hydroxyapatite and Hydroxyapatite-Based Ceramics. Available at: http://www2.chemia.uj.edu.pl/~skorska/Biomaterialy/hap/Orlovskii.pdf (Accessed September 4, 2017).
[9] Mostafa NY, Brown PW. Computer simulation of stoichiometric hydroxyapatite: Structure and substitutions. Journal of Physics and Chemistry of Solids. 2007;68(3):431-7.
[10] Teixeira S, Rodriguez MA, Pena P, De Aza AH, De Aza S, Ferraz MP, et al. Physical characterization of hydroxyapatite porous scaffolds for tissue engineering. Materials Science and Engineering: C. 2009;29(5):1510-4.
[11] Zobnenovice. review. (2017). Hydroxyapatite: properties, uses and applications | FLUIDINOVA. (online) Available at: http://zobnenovice.review/ (Accessed 25 Sep. 2017).
[12] Guo L, Huang M, Zhang X. Effects of sintering temperature on structure of hydroxyapatite studied with Rietveld method. Journal of Materials Science: Materials in Medicine. 2003;14(9):817-22.
[13] Thamaraiselvi TV, Prabakaran K, Rajeswari S. Synthesis of hydroxyapatite that mimic bone mineralogy. Trends Biomater Artif Org. 2006; 19(2): 81-83.
[14] Shikhanzadeh M. Direct formation of nanophase hydroxyapatite on cathodically polarized electrodes. J Mater Sci: Mater Med. 1998; 9: 67-72.
[15] Case Study: Polymer Matrix Composites in Automobiles, Available at: <https://www.princeton.edu/~ota/disk2/1988/8801/880110.PDF> (Accessed on 20th August 2017).
[16] Innovative Materials for Innovative Automobiles, Available at: < https://www.ceramtec.com/files/ca_innovative_materials_for_innovative_automobiles.pdf > (Accessed on 20th August 2017).
[17] Hapuhinna, H.; Gunaratne, R.; Pitawala, H. (2018), 'Development of a Biomaterial from Naturally Occurring Chloroapatite Mineral for Biomedical Applications', World Academy of Science, Engineering and Technology, International Science Index, Materials and Metallurgical Engineering, 12(8), 1827.
[18] Wei G, Ma PX. Structure and properties of nanohydroxyapatite/polymer composite scaffolds for bone tissue engineering. Biomaterials. 2004; 25(19): 4749-57.
[19] Composites in Automotive Applications: Review on brake pads and discs by Chrysoula A. Aza, Available at: <http://www.bristol.ac.uk/engineering/media/accis/cdt/news/aza.pdf> (Accessed on 20th August 2017).
[20] Ceramic Matrix Composites-Manufacturing and Applications in the Automotive Industry by Diego Bracho García, Available at: <http://www.bristol.ac.uk/engineering/media/accis/cdt/news/brachogarcia.pdf > (Accessed on 20th August 2017).
[21] Composite Manufacturing, Available at: <http://www.ae.iitkgp.ernet.in/ebooks/chapter3.html#kproj > (Accessed on 20th August 2017).
[22] Sphinxsai.com. (2010). Hydroxyapatite Synthesis Methodologies: An Overview. (online) Available at: http://sphinxsai.com/s_v2_n2/CT_V.2No.2/ChemTech_Vol_2No.2_pdf/CT=24%20(903-907).pdf (Accessed 25 Oct. 2010).
[23] Deptula A, Lada W, Olezak T, Borello A, Avani C, Dibartolomea A. Preparation of spherical powders of hydroxyapatite by sol gel processing. J Non-Cryst Solids. 1992; 147: 537-541.
[24] Li P, de Groot K. Better bioactive ceramics through sol-gel process. J Sol-gel Sci Technol.1994; 2: 797-801.
[25] Balamurugan, A., Kannan, S., Selvaraj, V. and Rajeswari, S. (2004). Development and Spectral Characterization of Poly(Methyl Methacrylate)/Hydroxyapatite Composite for Biomedical Applications. (online) Medind.nic.in. Available at: http://medind.nic.in/taa/t04/i1/taat04i1p41.pdf (Accessed 20 Dec. 2018).
[26] Heraeus.com. (2018). PALACOS R+G (high viscosity bone cement). (online) Available at: https://www.heraeus.com/kmedia/media/hme/doc_hme/products_me/palacos_bone_cement/r_rg_mv_mvg_lv_lvg/ifu/PALACOS_RG_IFU.pdf (Accessed 19 Dec. 2018).
[27] Irsmcascz. 2011. The Influence of CaO and P2O5 of Bone Ash upon the Reactivity and the Burnability of Cement Raw Mixtures. (Online). (31 July 2017). Available from: https://www.irsm.cas.cz/materialy/cs_content/2012/Ifka_CS_2012_0000.pdf.
[28] Hapuhinna, H., Gunaratne, R., Pitawala, H. (2018), 'Development of a Biomaterial from Naturally Occurring Chloroapatite Mineral for Biomedical Applications', International Journal of Chemical, Materials and Biomolecular Sciences, 11.0(8).
[29] Anon, 2015. Synthesis and modification of apatite nanoparticles for use in dental and medical applications. Japanese Dental Science Review. Available at: http://www.sciencedirect.com/science/article/pii/S1882761615000186 (Accessed September 9, 2017).
[30] Anon, (2018). Complex Analysis on Heat Treated Human Compact Bones. (online) Available at: https://www.researchgate.net/publication/267710992_Complex_analysis_on_heat_treated_human_compact_bones (Accessed 22 Feb.2018).